JOURNAL OF MATERIALS SCIENCE 2 (1967) 124–130

# Mechanical Properties of Selected Glass-Crystal Composites

W. J. FREY*, J. D. MACKENZIE
*Materials Engineering Department, Rensselaer Polytechnic Institute, Troy, New York, USA*

*Received 18 October 1966*

Desirable physical properties not provided by single-phase materials are often conveniently attained by multiphase composites. This paper is concerned with the variation of the mechanical properties of bulk glass through the incorporation of a crystalline oxide phase. Glass-$Al_2O_3$ and glass-$ZrO_2$ composites containing 20 and 40 vol % spherical, crystalline inclusions, 125 to 150 $\mu$m in diameter, were prepared by hot pressing. The effects of internal stress and elastic properties of the crystalline inclusion on composite mechanical properties were studied. Experimental elastic-property values agreed well with theoretical values calculated from Hashin's equations. Flexural strength tests of all composite compositions revealed that the fracture path rarely traversed the crystalline oxide inclusions. The $Al_2O_3$ and $ZrO_2$ additions strengthened the glass considerably, except when internal stresses were of sufficient magnitude to cause cracking of the glassy matrix upon cooling and before flexural testing. Glass-$Al_2O_3$ composites were consistently stronger than the glass-$ZrO_2$ counterparts. This strength difference is attributed to the higher elastic moduli of the $Al_2O_3$ composites. Hypotheses which postulate strengthening as a result of restricted flaw size are apparently not applicable to these materials.

## 1. Introduction

Experimentally observed strengths of bulk glass are generally several orders of magnitude less than the theoretically expected strengths. New techniques which may lead to the practical strengthening of glass are therefore of great interest. As outlined by Ernsberger [1], the majority of such techniques generate compressive stress on the glass surface, for instance, tempering, surface crystallisation, and ion exchange. Another logical approach is to vary the bulk properties of the glass by the addition of a second phase to form a glass-crystal composite.

In the present work, two crystalline oxides of relatively high elastic moduli and strength, $Al_2O_3$ and $ZrO_2$, were selected as the second-phase components for these composites. The objectives were to evaluate the strength and elastic properties of such composites as a function of: (i) the elastic properties of the components; (ii) the thermal expansion coefficients of the components; (iii) the degree of interfacial bonding between components; (iv) volume fraction of the crystalline phase.

## 2. Experimental Procedure

### 2.1. Sample Preparation

Two series of glass-crystal composites were prepared for this study, utilising commercially available glasses, and $Al_2O_3$ and lime-stabilised $ZrO_2$ as the two crystalline inclusions. Physical properties of these materials pertinent to this study are presented in table I. The series A composites, prepared to study the influence of inclusion elastic properties, contained 20 and 40 vol % of spherical, $Al_2O_3$, and $ZrO_2$ inclusions, 125 to 150 $\mu$m in diameter, dispersed in glass I. The series B composites, prepared to study the influence of internal stresses, contained 20 and 40 vol % of spherical, $Al_2O_3$ inclusions,

*This paper is based on part of a thesis submitted by W. J. Frey in partial fulfilment of the requirements for the degree of Master of Science in Materials, Rensselaer Polytechnic Institute, June 1966.

TABLE I Pertinent physical properties of composite components (1 lb/in.$^2$ = 7 × 10$^{-4}$ kg/mm$^2$).

| | Glass I 6810* soda zinc | Glass II 7740 borosilicate | Glass III 1990 potash soda lead | $Al_2O_3$ Norton 38 Alundum | $ZrO_2$ Norton Zirnorite I |
|---|---|---|---|---|---|
| Density (g/cm$^3$) | 2.65 | 2.23 | 3.47 | 3.91 | 5.65 |
| Strain point (°C) ($\log_{10}$ viscosity = 14.6) | 490 | 515 | 330 | — | — |
| Softening point (°C) ($\log_{10}$ viscosity = 7.6) | 770 | 820 | 500 | — | — |
| Melting point (°C) | — | — | — | 2000 | 2550 |
| Elastic modulus, $E$ (lb/in.$^2$ × 10$^{-6}$) | 9.4 | 9.1 | 8.4 | 55.0 | 20.3 |
| Linear coefficient of thermal expansion,** $\alpha$ (°C$^{-1}$ × 10$^{+6}$) | 6.9 | 3.3 | 12.4 | 5.47 | 8.85 |

*Corning glass code number.
**25 to 300° C for glasses; 25 to 500° C for $Al_2O_3$ and $ZrO_2$.

125 to 150 $\mu$m in diameter, dispersed in all three glasses. In table I, it is seen that the thermal expansion coefficients of these glasses are approximately equal to, lower than, and higher than that of $Al_2O_3$.

The glass powders used were less than 325 mesh or less than 45 $\mu$m. The spherical oxide particles were prepared by dropping angular particles of −100 +120 sieve fraction through an ac-powered, carbon arc. Selected spheres, 125 to 150 $\mu$m in diameter, were then dry mixed with the glass powders for at least 20 h in a double-cone blender. The powder mixtures were then hot pressed in graphite dies at 2500 lb/in.$^2$ (1 lb/in.$^2$ = 7 × 10$^{-4}$ kg/mm$^2$) for 25 min at a temperature of 50° C below the softening point of the particular glass used to give cylindrical samples, 0.50 in. in diameter and 0.75 in. in length (1.0 in. = 25.4 mm). Composite densities in excess of 97 % of theoretical were obtained for all samples.

One sample of each series A composite was prepared for ultrasonic elastic-property measurements by lapping its end faces parallel to within 0.0001 of an inch, and then gold plating it by vapour deposition to provide proper electrical grounding for ultrasonic measurements. Samples for flexural strength measurements were prepared by sectioning the as-pressed cylindrical samples, with a precision diamond saw, into discs 0.500 in. in diameter and 0.040 to 0.060 in. in thickness. Sample surface roughness was standardised by grinding the sample for 2 min on a cast-iron wheel in a slurry of water and 400-grit SiC abrasive powder.

## 2.2. Mechanical Property Measurements

Elastic property values of the series A composites were determined experimentally by an ultrasonic-pulse reflection technique, after Ahrens and Katz [2], utilising quartz-crystal transducers bonded to the end face of each cylindrical composite sample. The times necessary for longitudinal, and transverse, ultrasonic pulses to travel through each series A composite were determined at 5, and 9 Mhertz (1 hertz = 1 c/sec), respectively. These pulse travel-times were converted to wave velocities which were then used to calculate the elastic, bulk, and shear moduli of the composites.

The flexural strengths of 10 to 15 samples of each composite composition were determined on an Instron tensile tester with the special test fixture shown in fig. 1. Each disc-shaped composite sample was supported by the lower, circular knife-edge, and was then point loaded at the centre of its upper surface, thus putting its lower surface in tension. Curves of applied load versus sample deflection were recorded to failure, at a nominal crosshead speed of 0.002 in./min. The modulus of rupture of each sample was calculated with a modified form of Timoshenko's [3] equation for stress at the centre of the lower surface of a centrally loaded, thin disc.

$$\sigma_{max} = \frac{P}{h^2} [0.606 \log(a/h) + 1.13] \quad (1)$$

This equation was derived from Timoshenko's more general equation using a value of 0.25 for Poisson's ratio.

$$\sigma_{max} = \frac{P}{h^2} \{(1 + \nu) [0.485 \log(a/h) + 0.52] + 0.48\} \quad (2)$$

where: $\sigma_{max}$ = maximum tensile stress; $P$,

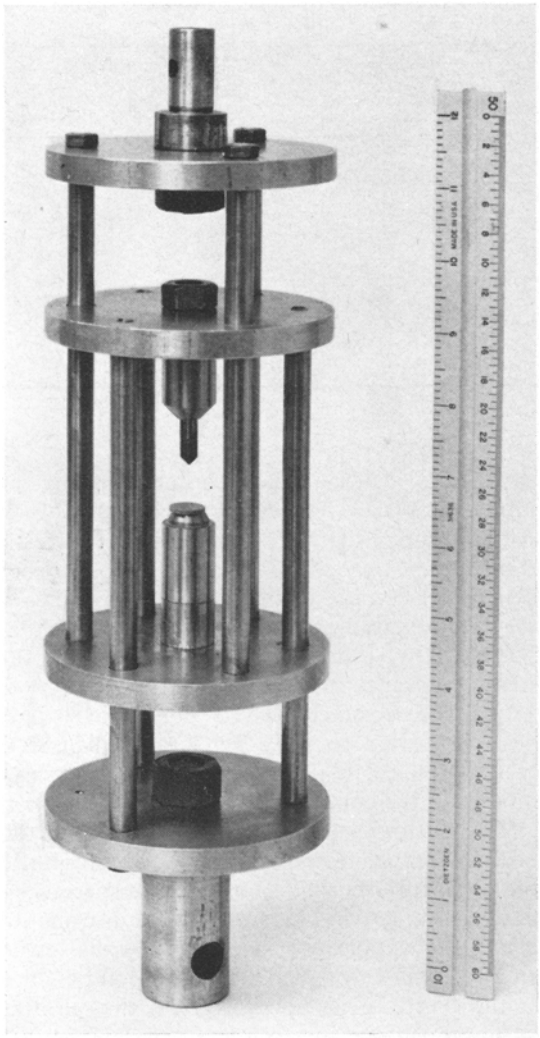

*Figure 1* Photograph of test fixture for flexural strength measurements.

applied load; $h$, disc thickness; $a$, radius of circular knife-edge; $\nu$, Poisson's ratio.

Since the disc sample geometry utilised for these flexural strength measurements was rather unconventional, a calibration was performed by comparing strength values obtained for disc samples tested on the circular knife-edge assembly with values obtained for conventional bar samples, of similar composition, fractured in four-point loading. Excellent agreement was obtained. Representative, whole, and fractured samples of each composite composition were ground and polished for observation of composite microstructure.

## 3. Results and Discussion

### 3.1. Composite Microstructure and Fracture

Photomicrographs of representative samples were taken before and after fracture to establish a basis for discussion of the effects that internal stresses, inclusion elastic properties, and glass-inclusion interfacial bonding had on the flexural strength and fracture of the composites.

Binns [4] reported that glass-$Al_2O_3$ composites with angular $Al_2O_3$ grains cracked upon cooling in cases where the thermal expansion coefficient of the glass was higher than that of the $Al_2O_3$. The present results show that this is also true for spherical inclusions. The composites with two glasses, one having an expansion coefficient slightly higher than, and the other lower than that of the $Al_2O_3$, showed no cracks (glasses I and II of table I; see, for example, fig. 2). On the other hand, composites made with glass III, the coefficient of expansion of which is appreciably greater than that of $Al_2O_3$, showed extensive cracking on cooling. Such cracks found in the glass III-$Al_2O_3$ composites are shown in fig. 3. These cracks apparently originated from internal stresses generated in the composite as it cooled from its fabrication temperature. High tangential stresses at the glass-$Al_2O_3$ interface are considered to be responsible for these matrix cracks. Such stresses were calculated for the case of a spherical inclusion using Selsing's [5] equation.

$$\sigma_x = -2\sigma_t = \frac{-(\alpha_m - \alpha_p)}{\frac{1+\nu_m}{2E_m} + \frac{1-2\nu_p}{E_p}} \left(\frac{R^3}{r^3}\right) \quad (3)$$

where: m = glass matrix; p, crystalline inclusion; $\sigma_x$ and $\sigma_t$, radial and tangential stresses; $\alpha$, linear coefficient of thermal expansion; $\Delta T$, decrease in temperature; $R$, inclusion radius; $r$, radial distance from centre of inclusion to a point in glass matrix; $\nu$, Poisson's ratio; $E$, elastic modulus. Stresses $\sigma_x$ and $\sigma_t$ at the glass III-$Al_2O_3$ interface were calculated to be 24800 and 12400 lb/in.$^2$ respectively.

In fig. 2, it is seen that some of the spherical $Al_2O_3$ inclusions were porous and sometimes hollow. This porosity was approximately 7 vol % from density calculations. The porosity apparently did not affect composite strength since post-fracture examination revealed that fracture paths rarely traversed the spherical particles. This is exemplified by fig. 4 for a glass I-40 vol %

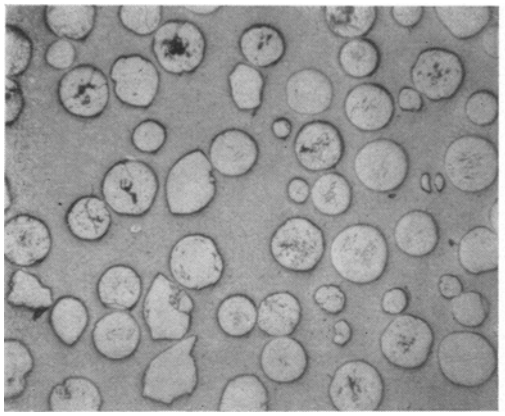

*Figure 2* Microstructure of glass I 40 vol % $Al_2O_3$ composite (×50).

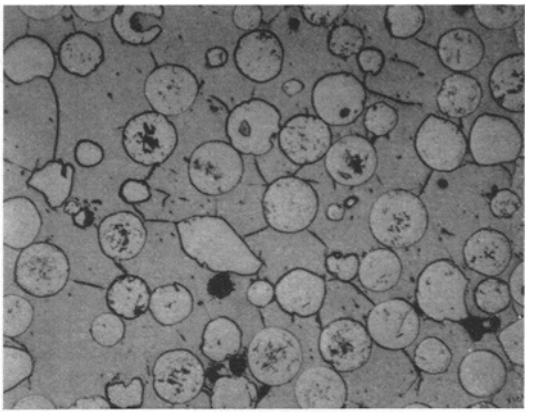

*Figure 3* Microstructure of glass III-40 vol % $Al_2O_3$ composite (×50).

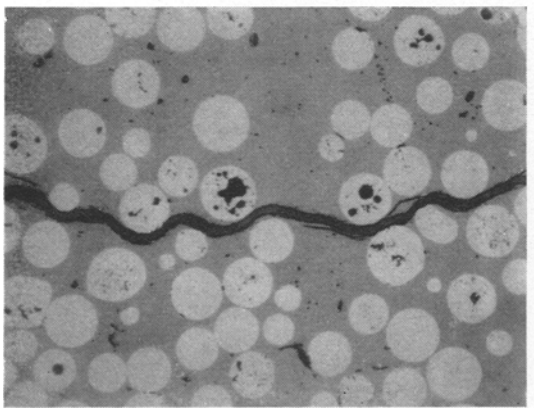

*Figure 4* Fracture path in glass I-40 vol % $ZrO_2$ composite (×50).

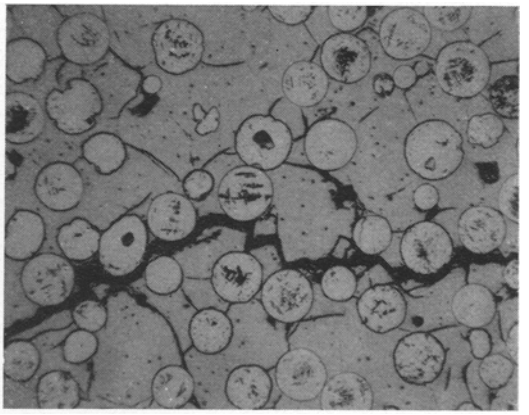

*Figure 5* Fracture path in glass III-40 vol % $Al_2O_3$ composite (×50).

$ZrO_2$ composite. Evidence of good interfacial bonding is shown by the adherence of the thin layer of the glassy matrix on the $ZrO_2$ inclusions, adjacent to the fracture path shown in fig. 4. No separation of the oxide spheres from the glassy matrix was observed after fracture and subsequent polishing. Failure of the glass III-$Al_2O_3$ composites, which contained cracks before testing, is characterised by a simple link-up of such cracks as shown in fig. 5. The difference in the fracture patterns in figs. 4 and 5 is apparent.

### 3.2. Elastic Properties

The mechanical behaviour of a glass-crystal composite is closely related to its elastic properties. Ideally, the elastic property values of a composite should be calculable from the elastic properties of the respective components. Hasselman and Fulrath [6], for instance, found that Hashin's [7] method for predicting the elastic properties of heterogeneous systems worked well for composite systems involving glass and tungsten. Hashin's method was similarly employed for the present systems. In table II, the experimentally observed values of shear, bulk, and elastic moduli are compared with those calculated for the series A composites. The agreement is within the limits of experimental error as shown in fig. 6.

### 3.3. Composite Flexural Strength

Composite flexural strength is affected by many factors. The important ones include: (i) thermal expansion differences of composite components; (ii) elastic properties of crystalline

TABLE II Calculated and experimental elastic properties of the series A composites (1 lb/in.$^2$ = $7 \times 10^{-4}$ kg/mm$^2$).

| | Volume fraction of dispersed inclusion | | | |
|---|---|---|---|---|
| | 0.2 $Al_2O_3$ | 0.4 $Al_2O_3$ | 0.2 $ZrO_2$ | 0.4 $ZrO_2$ |
| Shear modulus, $G_c$ (lb/in.$^2$ $\times$ $10^{-6}$) | | | | |
| Theory | 5.09 | 6.60 | 4.59 | 5.31 |
| Experiment | 4.96 | 6.75 | 4.37 | 5.39 |
| Bulk modulus, $K_c$ (lb/in.$^2$ $\times$ $10^{-6}$) | | | | |
| Theory | 6.52 | 8.60 | 6.03 | 7.32 |
| Experiment | 6.37 | 7.82 | 6.10 | 7.79 |
| Elastic modulus, $E_c$ (lb/in.$^2$ $\times$ $10^{-6}$) | | | | |
| Theory | 12.10 | 15.60 | 11.00 | 12.80 |
| Experiment | 11.80 | 15.70 | 10.60 | 13.10 |

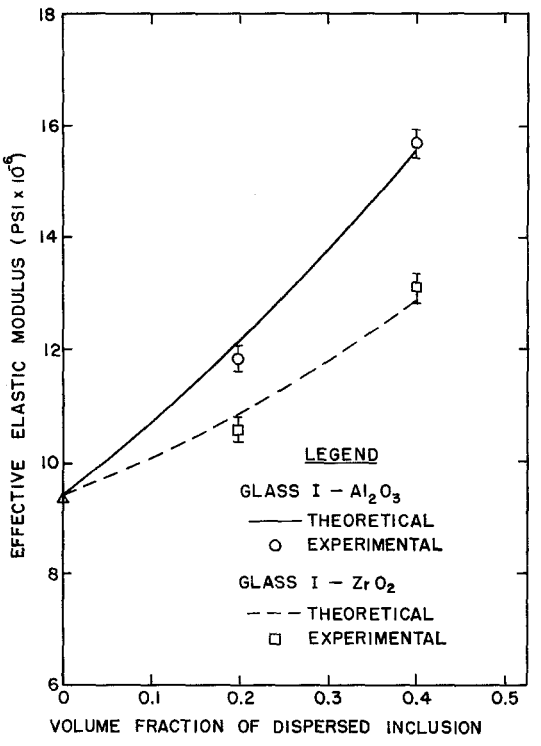


*Figure 6* Theoretical and experimental elastic moduli of glass I-$Al_2O_3$ and glass I-$ZrO_2$ composites. (In the illustrations, PSI is used instead of lb/in.$^2$ – 1 lb/in.$^2$ = $7 \times 10^{-4}$ kg/mm$^2$.)

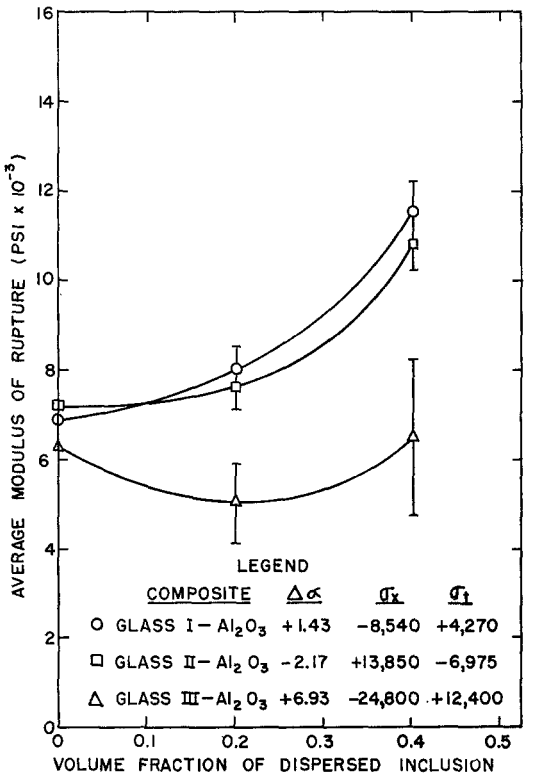


*Figure 7* Experimental moduli of rupture of series B glass-$Al_2O_3$ composites.

components; (iii) volume fraction of the inclusions. These factors are considered separately below.

### 3.3.1. Effect of Thermal Expansion Differences

The average moduli of rupture of the series B composites are presented in fig. 7. This figure gives the sign and magnitude of the thermal expansion difference ($\Delta\alpha$ in in./in. $^\circ$C $\times$ $10^6$) between composite components. A positive $\Delta\alpha$ indicates that the glassy matrix has a higher expansion than the $Al_2O_3$ inclusion. $\sigma_x$ and $\sigma_t$ are the radial and tangential stresses at the glass-crystal interface calculated with equation 3. A positive stress is tensile, while a negative stress is compressive. Both glass I and glass II were strengthened by the $Al_2O_3$ inclusions, even though internal stresses of considerable magnitude were present. Nason [8] obtained similar strengthening by adding spherical tungsten to glasses having higher and lower thermal expan-

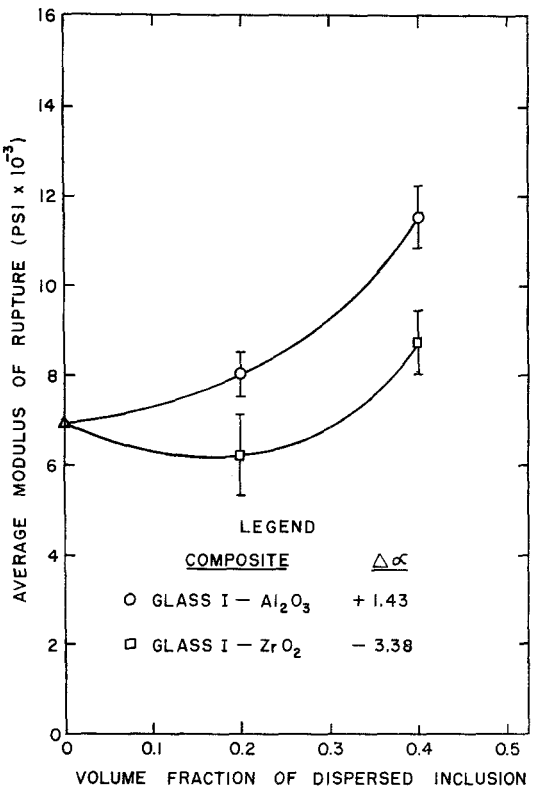


*Figure 8* Experimental moduli of rupture of glass I-$Al_2O_3$ and glass I-$ZrO_2$ composites.

sions than the tungsten inclusions. No statistically significant strengthening was observed for the glass III-$Al_2O_3$ composites. The lack of strengthening in this composite series is attributed to the cracks present in the glassy matrix before flexural strength tests were performed (see fig. 3). This hypothesis is supported by the characteristics of the fracture path shown in fig. 5. Thus internal stresses were found to reduce flexural strength only if they were large enough to cause premature fracture of the glassy matrix.

### 3.3.2. Effect of Inclusion Elastic Modulus

The flexural strength of the series A composites was measured to determine the effect of inclusion elastic modulus. As shown in fig. 8, the glass I-$Al_2O_3$ composites exhibited higher moduli of rupture than their glass I-$ZrO_2$ counterparts. Some difference between these composites must account for this difference in strength. Differences in internal stress did exist as indicated by the $\Delta\alpha$'s of different sign and magnitude in fig. 8. However, these stresses did not cause premature cracking in the glassy matrix as shown in figs. 2 and 4, and are thus considered to have a negligible effect on composite flexural strength. This is further supported by the results in fig. 7 for glasses I and II, where the $\Delta\alpha$'s are similar to those in fig. 8. Results of post-test examination of these samples, cited earlier in section 3.1, would eliminate any effects due to differences in the inclusion strength or interfacial bonding. All other parameters were identical for both composites, except for their elastic properties as shown in fig. 6. It is likely then that the predominant factor affecting the strength of these composites is their elastic modulus.

Crack initiation resulting in composite sample failure depends upon the sample deflection and the flaw-size distribution on the lower surface of the sample. Equal volume fractions of identical size fractions of $Al_2O_3$ and $ZrO_2$ inclusions in these composites eliminates variations in flaw-size distribution. Sample deflection per unit applied load is dependent on the composite's elastic modulus. Since the glass I-$Al_2O_3$ composites have substantially higher elastic moduli, larger loads must be applied to them to obtain deflections equal to those obtained for the glass I-$ZrO_2$ composites. If both composite types fail at equal disc deflections, the glass I-$Al_2O_3$ composites will fail at a higher applied load and will therefore have a higher flexural strength.

The deflection of a disc sample is related to its failure load via the elastic modulus and several geometrical constants, as shown in equation 4 given below.

$$D = 0.66 \frac{Pa^2}{E_c h^3} \tag{4}$$

where: $D$ = disc deflection; $P$, load; $a$, radius of circular knife-edge; $h$, disc thickness; $E_c$, composite elastic modulus. Indeed, the glass I-40 vol % $Al_2O_3$, and glass I-40 vol % $ZrO_2$ composites did fail at approximately equal deflections of $5.26 \pm 0.14 \times 10^{-3}$, and $5.04 \pm 0.26 \times 10^{-3}$ in., respectively.

Equation 4 may be used to obtain a nominal strength ratio for two composites which fail at equal deflections and contain equal volume fractions of identical size fractions of crystalline inclusions possessing different elastic properties. The predicted strength ratio for the glass I-40 vol % $Al_2O_3$ and glass I-40 vol % $ZrO_2$ composites is 1.20, which is approximately 10% below the observed strength ratio of 1.32. These results

indicate that inclusion elastic properties do affect composite flexural strength.

### 3.3.3. Effect of Inclusion Volume Fraction

The results in fig. 7 seem to indicate that the flexural strength of the glass-$Al_2O_3$ composites increases in a non-linear manner with increasing inclusion volume fraction. Both the increasing composite elastic modulus and decreasing distance between particles in the glassy matrix may contribute to this strengthening. An approximate calculation of the length of the Griffith-type flaw responsible for failure in a glassy sample with no inclusions can be made with the following equation:

$$\sigma_f = \frac{\sqrt{(4ES)}}{\pi C} \quad (5)$$

where: $\sigma_f$ = glass rupture strength; $E$, elastic modulus; $S$, surface energy; $C$, flaw length. For glass I, the average flaw length calculated is 140 $\mu$m. A convenient parameter for describing and calculating the average length of glassy phase between spherical particles distributed in a matrix is mean free path, $\bar{F}$, defined by equation 6 due to Fullman [9].

$$\bar{F} = \frac{4}{3}\frac{R(1 - V_p)}{V_p} \quad (6)$$

$R$ = inclusion radius and $V_p$ = inclusion volume fraction. The mean free paths of the glassy phase in the glass I-20 and 40 vol % $Al_2O_3$ composites was calculated to be 320 and 180 $\mu$m respectively. These are appreciably higher than the flaw size of 140 $\mu$m given by equation 5. Thus the restricted flaw mechanism postulated by Nason, and recently more fully developed by Hasselman and Fulrath [10], does not contribute to the observed strengthening of the present series of composites. However, the mean free path of the glassy phase can be significantly decreased when the inclusion particle size is reduced. The restricted flaw hypothesis is perhaps then applicable. Obviously, then, the increasing elastic properties of these composites with increasing volume fraction of $Al_2O_3$ must at least in part be responsible for the observed increase in strength.

## 4. Conclusions

In conclusion it may be stated that:

(*a*) The elastic properties of these glass-crystal composites can be satisfactorily predicted with Hashin's analysis.

(*b*) The $Al_2O_3$ and $ZrO_2$ inclusions in these composites offered considerable resistance to fracture, thus causing matrix fracture to predominate.

(*c*) Internal stresses due to thermal expansion differences do not degrade glass-crystal composite rupture strength, unless they cause premature cracking of the glassy matrix.

(*d*) These glass-crystal composites behave like constant strain systems, in that their rupture strength is dependent on their elastic moduli.

(*e*) The restrictive flaw mechanism due to Nason does not contribute to the strength increases observed in these composites with increasing inclusion volume fraction.

## Acknowledgements

The authors are grateful to R. S. Gilmore and T. Allersma for their assistance in the experimental work. This work was supported in part by the National Aeronautics and Space Administration under Contract No. NSG 100-60.

## References

1. F. M. ERNSBERGER, *Glass Ind.* **47** (1966) 481.
2. T. J. AHRENS and S. KATZ, *J. Geophys. Res.* **67** (1962) 2935.
3. TIMOSHENKO, "Theory of Plates and Shells" (McGraw-Hill, 1940), p. 70.
4. D. B. BINNS, "Science of Ceramics", Vol. 1 (Academic Press, 1962), p. 315.
5. J. SELSING, *J. Amer. Ceram. Soc.* **44** (1961) 419.
6. D. P. H. HASSELMAN and R. M. FULRATH, *ibid* **48** (1965) 548.
7. Z. HASHIN, *J. Appl. Mech.* **29** (1962) 143.
8. D. O. NASON, "Effect of Interfacial Bonding on Strength of a Model Two-Phase System", M.S. Thesis, University of California (1962).
9. R. L. FULLMAN, *Trans. AIME* **197** (1953) 447.
10. D. P. H. HASSELMAN and R. M. FULRATH, *J. Amer. Ceram. Soc.* **49** (1966) 68.